Photocatalytic Activity Assessment of Some Transition Metal Doped Titania Aerogels via Morpho-Structural Analysis

M. Popa*, L. Baia**, C. Ghica***, M. Baia**, E. Indrea****, V. Danciu*

*Faculty of Chemistry and Chemical Engineering, Babes-Bolyai University, 400028, Cluj-Napoca, Romania
**Faculty of Physics, Babes-Bolyai University, 400084, Cluj-Napoca, Romania
***National Institute for Research and Development of Materials Physics (INCDFM), P.O. Box MG-7/077125, Bucharest-Magurele, Romania
**** National Institute for Research and Development of Isotopic and Molecular Technologies, 400293 , Cluj-Napoca, Romania
vdanciu@chemubb.cluj.ro

ABSTRACT

Cu doped TiO_2, Ce doped TiO_2 and undoped TiO_2 aerogels were obtain in order to compare their photocatalytic activity. The doped and undoped aerogels were obtained by sol-gel process, followed by supercritical drying and thermal treatment. XRD, ESEM, bulk elemental analysis and BET analysis were performed in order to determine the morphological and structural proprieties of doped and undoped samples. Photocatalytic activity of the undoped TiO_2 aerogel was found to be the best. Cu- and Ce- TiO_2 aerogels exhibits a close photocatalytic activity.

Keywords: metal doped TiO_2, aerogel, photocatalysis, salicylic acid

1 INTRODUCTION

The polluted waters purification by using TiO_2 photocatalysts has many advantages regarding the environmental protection [1]. TiO_2 is a nontoxic and cheap semiconductor and has light absorption properties. Its band gap around 3.2 eV (anatase TiO_2) and 3 eV (rutile TiO_2) [2] allows TiO_2 an UV light absorption (~5% of solar spectrum) at 388 nm and 413 nm. Many authors considered TiO_2 a promising photocatalytic material [3, 4, 5]. However it needs improvement and optimizations considering heterogeneous photocatalytic applications. According to the literature, the enhancement of TiO_2 photocatalytic efficiency could be obtained by extending its light absorption in the visible region of the solar spectrum [6, 7], by increasing the recombination time of electron-hole pair [8]. Its photoactivity is also depending on crystalline structure, particles size, specific surface area, point of zero charge (PZC) [8], the presence of OH groups on the photocatalyst [9] etc. Doping TiO_2 with transition metal was widely employed in the last years. The presence of metals determines morphological, structural and electronic modifications in the TiO_2 lattice. At the electronic level, doping TiO_2 creates electronic states in TiO_2 band gap that act as trapping charge carriers and intercede in the interfacial transfer. Thus, the lifetime of photogenerated electron-hole pair is increased [8, 10]

Cu doped TiO_2 has been traditionally used for CO_2 photocatalytic reduction process. There are only some studies on the photo-oxidation process [8, 10, 11]. Ce doped TiO_2 was more investigated but its effect on the photocatalytic activity is still disputed [12, 13]. 0.5-1at % is considered the best metal concentration in TiO_2, considering their effect on photocatalytic activity [13, 14].

The presence of transition metal in TiO_2 matrix creates a controversial effect on the photocatalytic activity of TiO_2. However the efficiency of doped TiO_2 is depending on many factors such as synthesis process, method of doping, the type and doping concentration.[15]

The objective of this paper is to obtain 1at % of Cu-, Ce- doped TiO_2 and undoped TiO_2 aerogels and to compare them from morphological and structural point of view in order to conclude about the photocatalytic efficiency of these doped aerogels.

2 EXPERIMENTAL

2.1 Sample preparation

For the synthesis of copper and cerium doped and undoped TiO_2 gels were used: Ti(IV) isopropoxide (TIP) (>98%, Merck-Schuchardt), anhydrous ethanol (EtOH) (analytical grade, Aldrich), deionised H_2O and HNO_3 (analytical grade, 70%, Primexchim), $Ce(NO_3)_2 \cdot 6H_2O$ (Aldrich), $Cu(NO_3)_2 \cdot 3H_2O$ (Aldrich). The molar ratios were H_2O: TIP = 3.75, EtOH:TIP = 21 and HNO_3:TIP = 0.1. The corresponding molar ratios of $Me(NO_3)_x$/TIP are presented in Table 1. The synthesis was done at room temperature, with stirring. The supercritical drying of TiO_2 gels was performed in a SAMDRI-PVT 3D (Tousimis) critical point dryer, in the following conditions: 0.1 kg/min fill rate, 3.5 h purge time, 40 min. heat time, 1h maintained in supercritical conditions (100 atm, 40°C), 1h depressurize time. The obtained aerogels were thermal treated at 500°C

Clean Technology 2008, www.ct-si.org, ISBN 978-1-4200-8502-0

for 2h in air, using a CARBOLITE furnace, and then were morpho-structural characterized.

2.2. Sample characterization

The Brunauer-Emmett-Teller (BET) surface areas (S_{BET}) were derived from krypton physisorption measurements at 77 K using a glass home-made installation. Prior to measurements, the samples were degassed to 0.001 Pa at 448 K. S_{BET} was calculated in the relative pressure range of 0.05-0.3, assuming a cross-sectional area of 0.195 nm^2 for the krypton molecule.

X-ray Diffraction (XRD) measurements were performed using a BRUKER D8 Advance X-Ray diffractometer, working at 45 kV and 30mA. The Cu K_α radiation, Ni filtered, was collimated with Soller slits. The data of the X-ray diffraction patterns were collected in a step-scanning mode with $\Delta 2\theta = 0.02^0$ steps. Pure silicon powder standard sample was used to correct the data for instrumental broadening.

Bulk elemental analysis was performed using an inductively coupled plasma-mass spectroscope (ICP-MS).

Elemental analysis of the surface sample was performed by environmental scanning electron microscopy (ESEM) using an INCA x - sight microscope (model 6427 OXFORD INSTRUMENTS).

2.3. Photocatalytic activity

The photocatalytic activity of the doped and undoped TiO_2 aerogels was determined by monitoring the photodegradation of the salicylic acid as standard pollutant. Photodecomposition experiments were performed in a Teflon cell with a quartz window for UV illumination using a high pressure Hg lamp (250 W, HBO Osram). The photodegradation profile was obtained by spectrophotometrical determination (? = 295 nm) of the concentration of salicylic acid, using a Jasco V-530 spectrophotometer. The working temperature was $20\text{-}22^0$C and the solution pH 5.3. Before UV irradiation as well as before UV-Vis measurements, the cell with the sample was kept in dark for 15 minutes in order to achieve the equilibrium of the adsorption-desorption process.

3 RESULTS AND DISCUSSION

3.1. BET measurements

Table 1 lists the specific surface area (S_{BET}) of different TiO_2 aerogels, thermal treated at 500^0C, 2h. The metal doped TiO2 aerogels exhibit a decreasing of S_{BET} by 11-23% comparing with the undoped TiO2 aerogel. Ce doped TiO_2 presents a specific surface area slight bigger than Cu doped TiO_2 aerogel.

Sample	Ce-TiO_2	Cu-TiO_2	TiO_2	TiO_2 P25
$Me(NO_3)_x$/TIP (molar ratio)	0.575	0.618	-	-
S_{BET} [m^2g^{-1}]	116	101	131	53
Particle size [nm]	9.8	11	6.9	5.2
$<e^2>^{1/2}_{hkl} \times 10^3$	4.21	5.19	5.33	0.82
$10^3 \times k_{app}$ [min^{-1}]	7.69	7.59	12.9	2.5

Table 1: Specific surface area (S_{BET}), apparent rate constant, XRD crystalline particle size and average microstrain for the transition metal doped and undoped TiO_2 aerogel and TiO_2 Degussa P25, calcined at 773 K, 2h.

3.2. XRD measurements.

XRD measurements (Fig.1) reveal an anatase structure both of the doped and undoped TiO_2 aerogels. Unit cell parameters were calculated through Rietveld refinement using the PowderCell software.

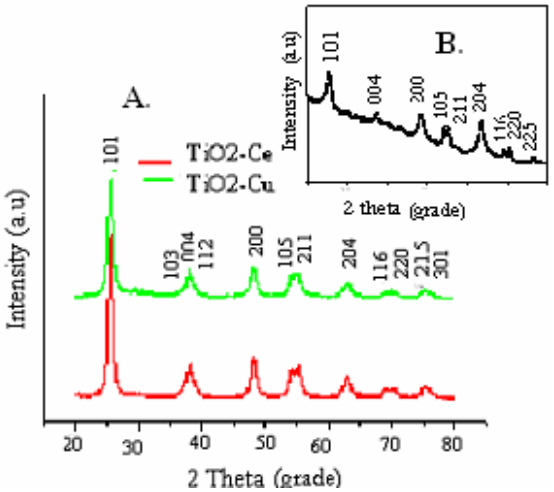

Figure 1: XRD difractogrames for: A.) Ce doped TiO_2 and Ce doped TiO_2 aerogels, B.) undoped TiO_2 aerogel

The microstructural information obtained by single X-ray profile Fourier analysis of the TiO_2 samples were the effective crystallite mean size, D_{eff}(nm) and the root mean square (rms) of the microstrains averaged along the [hkl] direction, $<e^2>^{1/2}_{hkl}$. The single (1 0 1) TiO_2 anatase and (2 0 0) TiO_2 anatase X-ray diffraction profiles were analyzed in order to determine the microstructural parameters of TiO_2 anatase structure [16, 17]. The Warren-Averbach X-ray profile Fourier analysis of the (1 0 1) TiO_2 anatase and (2 0 0) TiO_2 anatase peak profiles were processed by a XRLINE [18] computer program The particles size (Table 1) presents an increasing at the doped samples comparing with the undoped one. Ce doped TiO_2 aerogel particles presents a 1.4

times higher particle size and Cu doped TiO_2 aerogel presents 1.6 times higher. However, analyzing c parameter of the Cu doped TiO_2 crystalline cell (c = 0.9483 nm) and Ce doped TiO_2 crystalline cell (c = 0.9481 nm) with the undoped TiO_2 (c = 0.9486) no significant modification have been noticed. This could be explained as that the transition metal ions have not been incorporated in the TiO_2 lattice [19]. The quite high microstain average values, $\langle \varepsilon^2 \rangle^{1/2}_{hkl}$ (Tabel. 1) could indicate that the doped samples strain is due to an intergranular doped layer at the surface of the TiO_2 crystalline domains.

3.3. ESEM and ICP-MS measurements

The results of ESEM measurements (see tables 2 and 3) of the doped TiO_2 aerogels show the presence of doping metals on the surface of TiO_2 matrix. A non-uniform surface metal distribution in the Cu doped TiO_2 sample was revealed. Only in a single spectrum (spectrum 3) was identified the presence of copper. It could be concluded that Cu is agglomerated on the surface, probably in the stable oxidation state of CuO.

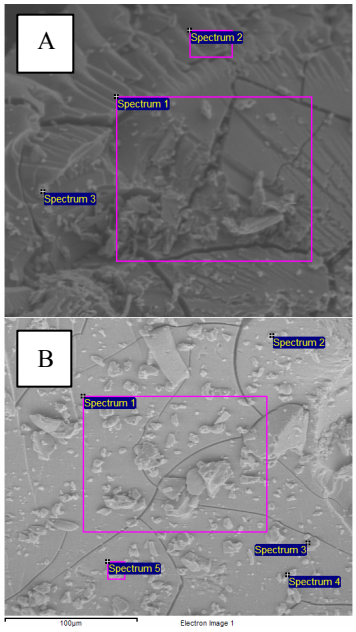

Figure 2: ESEM image: A) Cu doped TiO_2, B) Ce doped TiO_2

Spectrum	O	Ti	Cu	Total
1	49.17	50.83		100.00
2	50.55	49.45		100.00
3	51.67	47.52	0.81	100.00
Max.	51.67	50.83	0.81	
Min.	49.17	47.52	0.81	

Table 2: ESEM elemental determination on the Cu-TiO_2 aerogel surface

Spectrum	C	O	Ti	Ce	Total
1	2.39	34.06	58.60	4.20	100.00
2	2.04	41.58	52.62	3.76	100.00
3	2.57	35.91	57.08	3.88	100.00
4	2.60	35.79	57.09	4.10	100.00
5	2.49	35.96	58.06	3.49	100.00
Max.	2.60	41.58	58.60	4.20	
Min.	2.04	34.06	52.62	3.49	

Table 3: ESEM elemental determination on the Ce-TiO_2 aerogel surface

In the case of Ce doped TiO_2 aerogel it can be observed (see table 3) a more uniform surface metal distribution. The surface cerium mass percentage is about 3.88%, about five times higher than surface copper mass percentage. It probably exists as cerium oxide (CeO_2), as other authors remarked in Ce doped TiO_2 samples [15, 22].

Bulk elemental analysis, performed by ICP-MS, revealed the presence of 1 at % Cu in Cu -TiO_2 aerogel and 1.6 at % Ce in Ce-TiO_2 aerogel.

3.4. Photocatalytic activity determination

To evaluate the photocatalytic activity of the doped and undoped TiO_2 aerogels and TiO_2 Degussa powder, the plotting $\ln(C_0/C)$ *vs* time (Fig. 3) was used. The apparent rate constant of the salicylic acid photodegradation was determined from the slope of linear fit of the plot [20]. The apparent rate constant values presented in the table 1 exhibit that all the TiO2 aerogels have a 3-5 times higher photocatalytic activity than P25 TiO_2 Degussa powder. The undoped TiO_2 aerogel sample has a photocatalytic activity about 1.7 times higher that those of the metal doped aerogels. These results could be due to both its highest surface area (131 m^2/g) and its smallest particle size (6.9 nm). The higher surface area determine a better salicylic

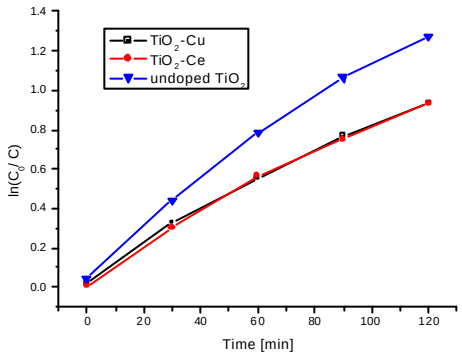

Figure 4: Photocatalytic properties of Cu doped TiO_2, Ce doped TiO_2 and undoped TiO_2 calcined at 500°C/2h, on salicylic acid.

Clean Technology 2008, www.ct-si.org, ISBN 978-1-4200-8502-0

acid adsorption [21] and the small particle size favors the switch over of the photogenerated carriers of TiO_2 to adsorbed water/organic compound molecules [12].

Ce doped TiO_2 aerogel presents an insignificant increasing of photoactivity comparing with Cu doped TiO_2 aerogel although has a higher surface area and a smaller crystallite size. The presence of a higher metal concentration (~1.6 at % Ce) than 1% could explain the insignificant increasing of its photocatalytic activity.

The surface homogeneous distribution of CeO_2 on TiO_2 aerogel probably hinder the OH• radical development and also partial block the adsorption centers of the aerogel destined to the organic compound. These can lead to a lower photocatalytic activity comparing with the undoped TiO_2 aerogel. It is known that the photocatalytic efficiency is strongly tied by the formation of Ti^{4+}-OH• radicals in photocatalytic process. According to Coronade et al. [22] the photogenerated holes could stabilize in Ti^{4+}-O^-, in the CeO_2 /TiO_2 photocatalysts , which apparently does not favor the photocatalytic process.

Further studies are necessary in order to clarify the influence of the type and the doping concentration on the morpho-structural properties of TiO_2. The photogenerated electron-hole recombination time, XPS analysis for real determination of metal state in the doped TiO_2, the determination of surface OH groups concentration, UV-VIS absorbance are needed to be perform in order to draw a clear conclusion about doped and undoped aerogels.

4 CONCLUSIONS

1at% Cu doped TiO_2 and 1.6at % Ce doped TiO_2 and undoped TiO_2 aerogels were obtained. The morphological and structural properties were analyzed, using different techniques. XRD analysis revealed a crystalline structure of anatase in all TiO_2 aerogel samples. The particles size increase of 1.4 - 1.6 times, due to the doping process. ESEM analysis showed that the distribution of the metal oxide, which could form on the surface of the doped samples, is relatively uniform. Photocatalytic activity of Cu doped TiO_2, Ce doped TiO_2 and undoped TiO_2 aerogels on salicylic acid degradation was performed. We found that the undoped TiO_2 aerogels exhibits the best photocatalytic activity. The presence of metal dopants in TiO_2 lattice decreases its photocatalytic activity because of the metal oxides formation on the surface of the TiO_2. This determines a blockage and reduces the number of OH• radicals . However all obtained TiO_2 aerogels exhibits a better photocatalytic activity comparing with P25 TiO_2 Degussa

REFERENCES

[1] A. Fujishima, T.N. Rao, D.A. Tryk, J. Photochem. Photobiol. C 1, 1-21, 2000.

[2] S. Boujday, F. Wunsch, P. Portes, J. F. Bocquet, C. Colbeau - Justin, Solar Energy Materials & Solar Cells, 83, 421-433, 2004.

[3] U. Diebold, Surface Science Raports, 48, 53, 3003.

[4] A.L. Linsebigler, G.Q. Lu, J. T. Yates, Chem. Rev., 95, 735, 1995.

[5] Gonghu Li, Kimberly A. Gray, Chem. Phys. 339, 173-187, 2007.

[6] H. Wei, Y. Wu, N. Lun, F. Zhao, J. Mat. Sci., 39, 1305-1308, 2004.

[7] R Asahi, T. Morikowa, T Ohwaki., K Aoki., Y Taga, J. Mat. Sci., 293, 2001

[8] A. Di Paola, E. Garcia-Lopez, S. Ikeda, G. Marci, B. Ohtani, L. Palmisano, Catal.Today, 75, 87-93, 2002.

[9] J.A. Rob van Veen, Fred T.G. Veltmaat, G. Jonkers, J. Chem. Soc., Chem. Commun, 1656-1658, 1985.

[10] G. Colon, M. Maicu, M.C. Hidalgo, J. A. Navio, Appl. Catal. B: Environ., 67, 41-51, 2006.

[11] E. Celik, Z. Gokcen, N. F. Ak Azem, M. Tanoglu, O.F. Emrullahoglu, Mater. Sci. Eng. B, 132, 258-265, 2006.

[12] J. Xiao, T. Peng, R. Li, Z. Peng, Ch. Yan, J. Solid Sate. Chem., 179, 1161-1170, 2006 .

[13] Y. Xu, H. Chen, Z. Zeng, B. Lei, Appl. Surf. Sci., 252, 8565-8570, 2006.

[14] T. Morikawa, Y. Irokawa, T. Ohwaki, Appl. Catal. A: 314, 123-127, 2006.

[15] J. Xiao,T. Peng, Ran Li, Z. Peng, Ch. Yan, J. Solid State Chem, 179, 1161-1170, 2006.

[16] J.G.M. van Bercum, A.C. Vermeulen, R. Delhez, T.H. de Keijser, E.M. Mittemeijer, J. Appl. Phys., 27, 345-353, 1994.

[17] E. Indrea and Adriana Barbu, Appl. Surf. Sci., 106, 498-501, 1996.

[18] N. Aldea, E. Indrea, Comput. Phys. Commun., 60, 155-159, 1990.

[19] C.Adan, A. Bahamonde, M. Fernandez-Garcia, A. Martinez-Arias, Appl. Catal. B: Environ., 72, 11-17, 2007

[20]A. Barau, M. Crisan, M. Gartner, A. Jitianu, M. Zaharescu, A. Gh ita, V. Danciu, V. Cosoveanu, I. Marian, J. Sol-Gel Sci. Techn., 37, 175, 2006.

[21] A.J. Maira, J.M. Cronado, V. Augugliario, K.L. Yeung, J.C. Conesa, J. Soria, J. Catal., 202, 413-420, 2001

[22] J.M. Coronado, A.J. Maira, A. Martinez-Arias, J.C. Conesa, J. Soria, J. Photochem. Photobiol., 150, 213-221, 2002